DISCLAIMER

This contractor document was prepared for the U.S. Department of Energy (DOE), but has not undergone programmatic, policy, or publication review, and is provided for information only. The document provides preliminary information that may change based on new information to be used specifically for Total System Performance Assessment analyses. The document is a preliminary lower-level contractor document and is not intended for publication or wide distribution.

Although this document has undergone technical reviews at the contractor organization, it has not undergone a DOE policy review. Therefore, the views and options of authors expressed may not state or reflect those of the DOE. However, in the interest of the rapid transfer of information, we are providing this document for your information per your request.

Interim Report to TWR

"Stress Corrosion Crack Growth Measurements in Environments Relevant to High Level Nuclear Waste Packages"

Peter L. Andersen
GE Corporate Research & Development Center
January 14, 2000

Interim Report to TWR

"Stress Corrosion Crack Growth Measurements in Environments Relevant to High Level Nuclear Waste Packages"

Peter L. Andresen
GE Corporate Research & Development Center
January 14, 2000

Overview

This program is designed to characterize the stress corrosion cracking response of waste canister structural materials for the Yucca Mountain Project. The waste package is one of the few elements of the project that can be engineered, and the ability to provide very long waste package lifetimes that can be predicted with confidence is a central factor in the release rate of radionucleides from the mountain.

General and localized corrosion, and stress corrosion cracking represent the most likely degradation modes for the waste package structural materials. The key to demonstrating and predicted the long waste package lifetimes lies in characterizing the local environment that forms on the waste package. This is particularly important for temperatures above ≈ 75 °C, where the heat flux through the waste package is higher, the environments more concentrated, and the material susceptibility to corrosion degradation is highest. Since the waste package is always hotter than its surrounding environment, probably by several °C at 75 – 120 °C, which translates into solution concentration on the waste package surface of at least several molar , and obviously a concentrated solution as the waste package initially cools to the temperature of the maximum boiling point elevation (of perhaps 120 °C). As the Yucca Mountain water drips or splashes onto the waste package and concentrates, its pH is expected to rise to at least 10, and perhaps much higher.

Other programs are addressing the general and localized corrosion in these and related environments. The objective of this program is to measure the stress corrosion crack growth rates under conditions that are both relevant and likely to promote stress corrosion cracking, i.e., fairly high concentrations at fairly high temperature.

Experimental Procedures

This program has utilized fracture mechanics, crack growth rate (1-inch compact type, or 1TCT) specimens of Alloy 22 and titanium grade 7; subsequent tests may evaluate titanium grade 16 and perhaps type 316 NG stainless steel. Materials were supplied in specimen form by the Project in the solution annealed conditions. To date, all materials have been tested in the as-received condition as provided by TWR.

Each specimen was fatigue pre-cracked in air, with the ending phase at the K_{max} used for SCC testing (30 MPa$\sqrt{m}$) at a load ratio R of 0.7. Each specimen was then assembled in an autoclave and tested in the specified chemistry at the corrosion potential. Both solution annealed Alloy 22 and titanium grade 7 were tested at 30 MPa$\sqrt{m}$. A complete transition from fatigue pre-cracking conditions to stress corrosion cracking conditions was made by continuing the cycling (generally at a load ratio R = 0.7) at a very low frequency (0.001 Hz) and eventually to increasingly long hold times at K_{max}. "Gentle" unloading cycles are used to help ensure that optimal results are obtained [1-2].

Careful selection of the environments to be evaluated is crucial, because the stress corrosion cracking results may be highly biased if, e.g., pitting or crevice corrosion occurs. These initial tests were performed in water that simulates the concentrated environment that must form on a hot waste package (net heat flux from the waste package means that the local environment is always concentrated, if not saturated). The mix of chemicals used for the test chemistry (specified by TRW) is shown below:

10.6 g Na_2CO_3 (anhydrous)
9.7 g KCl
8.8 g NaCl
0.2 g NaF
13.6 g $NaNO_3$
1.4 g Na_2SO_4 (anhydrous)
4.1 g $Na_2SiO_3*9H_2O$
55.3 g H_2O

In the first test (c143), the chemicals were mixed with water that had been heated to the boiling point in the autoclave. However, the recipe provided by TWR did not fully dissolved in water, leaving some solids in the autoclave. For the second test (c144), the chemicals were mixed with water maintained at the boiling point in a Teflon beaker for ≈ 60 minutes, then the solution (not the solids) were poured into the autoclave. A Hastelloy C-276 autoclave body was used for the Alloy C22 specimen; a commercial purity titanium autoclave was used for the titanium grade 7 specimen. Solution was sampled from the autoclaves during the test, as presented in the Results and Discussion section.

Control of dissolved oxygen is important, and near the boiling point of a solution the dissolved gas concentration varies markedly with temperature. To avoid extreme variations (and very low average dissolved oxygen concentrations), slowly flowing laboratory air was kept pressurized at 5 psig throughout the test. The exact concentration of dissolved oxygen can only be estimated. While the solubility of dissolved oxygen at 110 °C is well known in pure water [3], the "salting out" effect of this particularly chemistry and at 110 °C is not precisely known. Assuming that the "salting out" effect decreases the dissolved oxygen concentration by 2X compared to pure water (the solubility of O_2 in 110 °C water is 25.6 ppm per atmosphere partial pressure of O_2), the dissolved oxygen concentration should be about 0.91 ppm (25.6

ppm x 20.9% O_2 in air x 5 psi / 14.7 psi/atm divided by 2 for the "salting out" effect).

To prevent evaporative loss of water, a four foot long tube-in-tube heat exchanger was used, with cooling water on the outside. A back pressure regulator at the outlet of the autoclave gas space was used to maintain the desired (5 psi) system pressure. The water level in the autoclave was checked periodically by checking for continuity between the autoclave and an insulated stainless steel feed-through bar, and by occasional visual inspection which entailed a brief depressurization of the system. No water addition was needed.

Measurements of corrosion potential are complicated by the operation of the system near the boiling point. Thus, the solution in traditional internal or external Ag/AgCl electrodes containing 0.01 or 0.1 N KCl would boil at 110 °C, and zirconia membrane reference electrodes have very high resistivity at <200 °C. Thus, a modified external Ag/AgCl reference electrode was used which employed a 4 N KCl solution. Analysis of these data are not complete, and they will be presented in the next report.

Crack length was monitored in-situ using a reversing dc potential drop technique, as shown schematically in Figure 1.

Results and Discussion

Specimen c143 of titanium grade 7. An overview of the air fatigue and stress corrosion cracking results is shown in Figure 2. Following air fatigue precracking and assembly into the autoclave, the specimen was held at 11 MPa$\sqrt{m}$ while the temperature controller was tuned to provide good stability vs. time and adjustments were made to the air pressurization system (bubbling of laboratory air through the autoclave solution was initially attempted, but the tube used for bubbling was repeatedly sealed off by encrustations of salt).

An overview of the test is shown in Figures 3 and 4. Figure 3 shows the raw (point by point) data, as stored in the digital record, while Figure 4 shows the data using a 10-point moving average. Since the test segments that will be discussed are all comprised of many hundreds (typically 400 – 1200) of data points, the use of a moving average is fully justified and serves well its intended purpose of damping the effects of temperature fluctuations on indicated crack length. The dc potential drop crack monitoring system exhibited higher sensitivity to slight fluctuations in test temperature, markedly more so than we experience in our 288 °C testing.

As shown in Figures 3 – 5, at 277 hours the specimen was loaded to 30 MPa$\sqrt{m}$ and a very low frequency cycle was imposed at R = 0.7 and 0.001 Hz. Following an initial period of high growth rate, the growth rate became quite well behaved at $\approx 8 \times 10^{-8}$ mm/s (Figure 5). At 1555 hours into the test, the loading was modified by introducing a 1,000 hold time at K_{max} (making the duration of the hold time and the full cycle the same). This had little effect on crack growth rate, although the crack growth rate did slow down very slightly. Figure 5 (and the other figures that detail

specific test segments) show the linear regression fits over the duration of the test segment graphed, along with the calculations for the best fit slope (growth rate), the slopes corresponding to the upper and lower 95% confidence level, and the correlation coefficient (R^2). The high correlation coefficient (1.0 represents a perfect correlation) and the very close agreement of the upper and lower 95% confidence slopes provide a high level of confidence in the quality of the observations.

At 2154 hours, a longer hold time (9,000 s) at K_{max} was initiated (Figures 3, 4 and 6). This produced a decrease in crack growth rate of about 2X. The subsequent response was quite well behaved (Figure 6), although some tendency for the crack growth rate to decrease vs. time is evident. Nonetheless, when the entire data set shown in Figure 6 is evaluated, a good fit and high correlation coefficient are obtained, and the closeness of the upper and lower 95% confidence slopes strongly support the best fit crack growth rate of 4.0×10^{-8} mm/s.

At 2848 hours, a yet longer hold time (85,400 s) was introduced, yielding one unloading cycle per day (Figures 3, 4 and 7). Again, a relatively crisp and well-behaved response was observed, with a best fit crack growth rate of 1.6×10^{-8} mm/s. At 3713 hours, the specimen was unloaded (but not cooled down) because of concern for power outages as the threshold into the year 2000 was crossed. On re-loading, a small, short-term transient was observed (Figures 3 and 4), which is not unusual given the deep loading cycle. While we anticipate that the subsequent response will be similar to the prior response, the linear regression calculations have (for now) not included this transient period. The 1.6×10^{-8} mm/s growth rate is probably a good representation of the static load behavior of an "actively growing" stress corrosion crack. The distinction "actively growing" is crucial, because round robins [1,2] and other studies [4,5] have shown that that there are many cases where cracks don't grow or temporarily cease growing that are "anomalous" – i.e., in many other cases under identical conditions, well-behaved, long-term crack growth is obtained.

An extensive evaluation of crack growth data in nickel base alloys by a group of international experts [6] concluded that among the many experimental flaws in the available crack growth data, the failure to make a complete transition from fatigue precracking (which is transgranular and has different plastic zone characteristics than a stress corrosion crack) to an SCC crack is crucial, as is the use of at least occasional partial unloading to maintain an active crack. A more detailed discussion of the origins and implications of this phenomenon has been made [7], which hypothesized that the large differences in observed "K_{Iscc}" among different laboratories and investigators is associated with both experimental problems and the inherent probabilistic nature of both SCC initiation and growth. Since few specimens / sites / microstructures can be evaluated in the lab (compared to the available opportunities in actual structures), it is crucial to quantify dependencies and overall susceptibility by maintaining an active crack, or else the vast noise / scatter in the data overwhelm the dependencies [1,2,5-7].

However, it is equally important to recognize that "active" SCC is not necessarily easy to maintain, and there is strong experimental evidence to suggest that the probability

of maintaining "active" SCC (which is much higher than the probability of re-initiating SCC for a crack that has stopped) is related to the crack growth rate (fast cracks are much more likely to sustain their advance vs. time) and factors such as the creep rate, yield strength, etc. Compared to typical light water reactor operating temperatures of 274 to 340 °C (where extensive studies have been perfomed), the probability of sustaining SCC is significantly lower at ≤ 110 °C. Another very important factor is the incidence of "transients" such as start up and shutdown, vibrations, changes in plant output, etc. that (like partial unloading) can induce crack re-initiation. In this regard, there has undoubtedly never been an human design that will operate under more fully static conditions that the Yucca Mountain repository, because (barring the occurrence of exceedingly unlikely and rare incidents, such as earthquakes) the system will change (cool) only in a *very slowly*, well controlled fashion involving thermal changes of perhaps < 1 °C per century once the waste package cools sufficiently to have an aqueous environment (e.g., <120 °C). This should provide a remarkably low probability of stress corrosion cracking, especially given the low growth rates that are already measured, which will be dramatically lower still at stress intensity factors relevant to the development of cracks (e.g., << 10 MPa√m).

At 877 h into the test, the autoclave solution was sampled then submitted to the Materials Characterization Laboratory at GE Corporate R&D Center. The results are shown in Table1, and differ somewhat from the analysis of the solution used in test c144, perhaps because the undissolved solids were not left in the autoclave in c144.

The sample liquid was stored, and then recently used to evaluate the room temperature and 100 °C pH of the test solution. After calibration and checks in two buffered solutions, the pH was measured at room temperature to be 13.43. The vial containing the relatively small volume (about 25 cc) of solution was then heated in a beaker of boiling water, and the pH at about 100 °C was found to be 12.2 – 12.3. Note that the boiling point of this liquid is above 110 °C, so heating to 100 °C did not produce boiling (or even consequential evaporation during the short measurement). While this is not completely representative of the autoclave test solution, which is at 110 °C, the difference should be very small indeed.

Specimen c144 of Alloy C22. An overview of the air fatigue and stress corrosion cracking results for Alloy C22 is shown in Figure 8. Following air fatigue precracking and assembly into the autoclave, the specimen was left unloaded while adjustments were made to the temperature controller.

At 247 hours, the specimen was loaded to 11 MPa√m to equilibrate the dc potential drop system at the 110 °C test temperature. At 272 hours, the specimen was loaded to 30 MPa√m and a very low frequency cycle was imposed at R = 0.7 and 0.001 Hz (Figures 9 and 10). As with specimen c143, Figure 9 presents the raw, point-by-point data, while Figure 10 uses a moving average of 10 data points to smooth out the minor crack length fluctuations from temperature.

Because there was little initial evidence of crack advance, at 345 hours the load ratio R was lowered to 0.5, at which point crack advance commenced, although at a relatively low growth rate of $\approx 2.5 \times 10^{-8}$ mm/s (Figures 9 and 10). At ≈ 600 hours, there is a dip in the crack length vs. time signal that cannot be explained based on any change in the test conditions. The noise in the crack length vs. time signal was of lower periodicity (about 24 hours, perhaps from slightly greater fluctuations in room temperature) than for specimen c143. The subsequent response was well-behaved, as shown in Figure 11. At 1184 hours the loading was changed to R = 0.6, 0.001 Hz; this initially produced little discernible change in the growth rate. Over the time interval shown (including some data at R = 0.6), the linear regression fit was evaluated to be 2.1×10^{-8} mm/s. Additionally, detailed calculations for the best fit growth rate, the growth rates corresponding to the upper and lower 95% confidence levels, and the correlation coefficient (R^2). The high correlation coefficient and the close agreement of the upper and lower 95% confidence values provide a high level of confidence in the quality of the observations.

About 100 hours after making the change to R = 0.6, the crack growth rate apparently stopped (Figures 9 and 10). Because of this, a change was made at 1801 hours into the test from 0.001 Hz to 0.003 Hz. This was sufficient to re-activate the crack (Figures 9, 10 and 12) and produce well-behaved crack growth response for the subsequent 300+ hours. The best fit growth rate was 3.3×10^{-8} mm/s, with a very high correlation coefficient (R^2) of 0.988. Note that despite the increase in frequency by 3X, the growth rate only increased by about 60%, indicating a very strong environmental component of crack advance (if the crack were advancing by inert fatigue, its rate would be linear with frequency).

At 2137 hours, the frequency was returned to 0.001 Hz, and now the crack growth rate was sustained (Figures 9, 10 and 13). At 2481 hours, the load ratio was increased to R = 0.65, and again the growth rate was sustained. Finally, at 3345 hours the specimen was unloaded (but not cooled down) out of concern for power outages as we entered the year 2000. However, no problems were encountered and, on re-loading, the crack growth rate has been identical to the prior period.

While still fairly "gentle", the cyclic unloading currently used is still more aggressive than that currently used with specimen c143. This is consistent with the lower growth rates observed for Alloy 22 (compared to titanium Grade 7 for specimen c143); that is, the propensity for "active cracking" to cease increases as the growth rate decreases. We are planning to continue to increase the load ratio, R, and introduce hold times. Estimates of the growth rate under static conditions of "active cracking" can be made from experience and from comparison with the data from specimen c143. Using a factor of 4 as a reasonable estimate, the expected / estimated growth rate for Alloy 22 under static loading conditions might be between $1 - 2 \times 10^{-9}$ mm/s, a low number indeed, and more difficult still to measure than the rates observed to date. The importance and interpretation of "active crack" advance was addressed in the discussion of specimen c143.

At 507 h into the test, the autoclave solution was sampled then submitted to the Materials Characterization Laboratory at GE Corporate R&D Center. The results are shown below, and differ somewhat from the analysis of the solution used in test c143, perhaps because the undissolved solids were not left in the autoclave of this test.

As with specimen c143, the sample liquid was stored, and then recently used to evaluate the room temperature and 100 °C pH of the test solution. After calibration and checks in two buffered solutions, the pH was measured at room temperature to be 13.42. The vial containing the relatively small volume (about 25 cc) of solution was then heated in a beaker of boiling water, and the pH at about 100 °C was found to be about 12.6. Note that the boiling point of this liquid is above 110 °C, so heating to 100 °C did not produce boiling (or even consequential evaporation during the short measurement). While this is not completely representative of the autoclave test solution, which is at 110 °C, the difference should be very small indeed.

References

1. P.L. Andresen, "IGSCC Crack Propagation Rate Measurement in BWR Environments: Executive Summary of a Round Robin Study", SKI Report 98:27, ISSN 1104-1374, ISRN SKI-R-98/27-SE, SKI, Stockholm, 1999.

2. P.L. Andresen, K. Gott and J.L. Nelson, "Stress Corrosion Cracking of Sensitized Type 304 Stainless Steel in 288C Water: A Five Laboratory Round Robin", Proc. Ninth Int. Symp. on Environmental Degradation of Materials in Nuclear Power Systems - Water Reactors, AIME, 1999.

3. D.M. Himmelblau, J Chem Eng Data 5, 10, 1960.

4. P.L. Andresen, "Effects of Testing Characteristics on Observed SCC Behavior in BWRs", Paper #98137, Corrosion/98, NACE, 1998.

5. P.L. Andresen, "SCC Testing and Data Quality Consideration", Proc. Ninth Int. Symp. on Environmental Degradation of Materials in Nuclear Power Systems - Water Reactors, AIME, 1999.

6. Unpublished results from P.L. Andresen and other in an EPRI sponsored, international experts "PEER" group which evaluated crack growth data for Alloy 600 and Alloy 182 weld metal, 1999.

7. P.L. Andresen, "Probabilistic Interpretation of SCC Initiation & Growth", Paper #99446, Corrosion/98, 1999.

Table 1. The concentration of ions in the samples (ppm).

Ion	c143 - 9/3/99	c144 - 9/3/99
Sodium	130794	140322
	140412	139931
Potassium	56387	67651
	58772	71569
Fluoride	<145	<145
	<145	<145
Chloride	95989	101331
	91472	99920
Nitrate	101366	112752
	96497	105970
Sulfate	6249	5528
	6482	5976
Sulfur (33% of sulfate)	2107	1819
	2185	1968

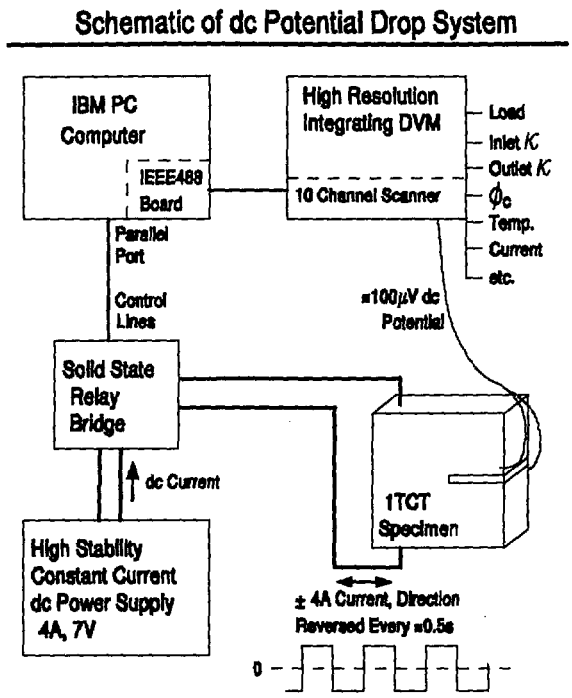

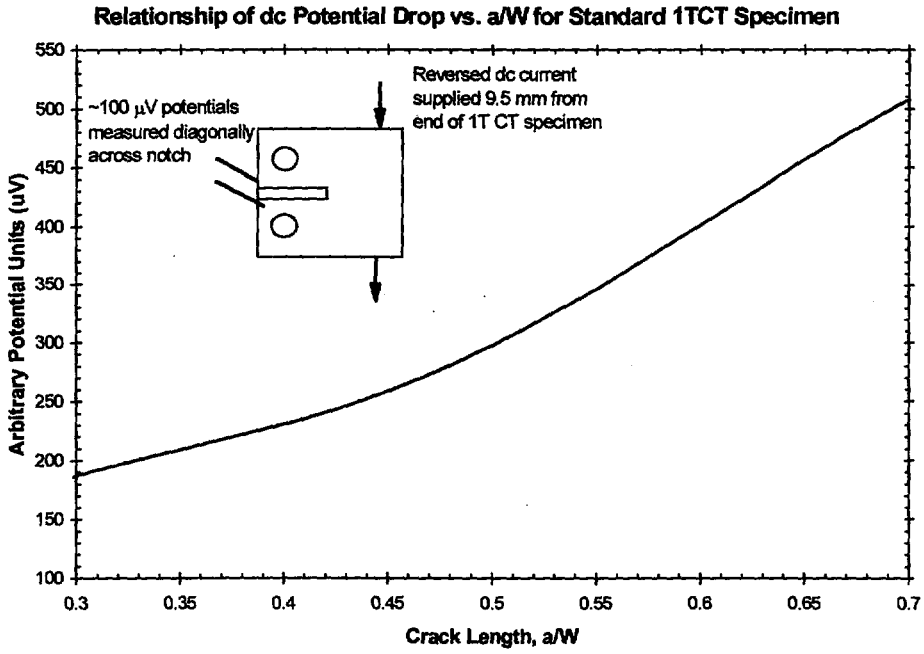

Figure 1. Schematic of (a) the computer control of current reversal, data acquisition, and data averaging techniques, and (b) the relationship between measured potential and crack length.

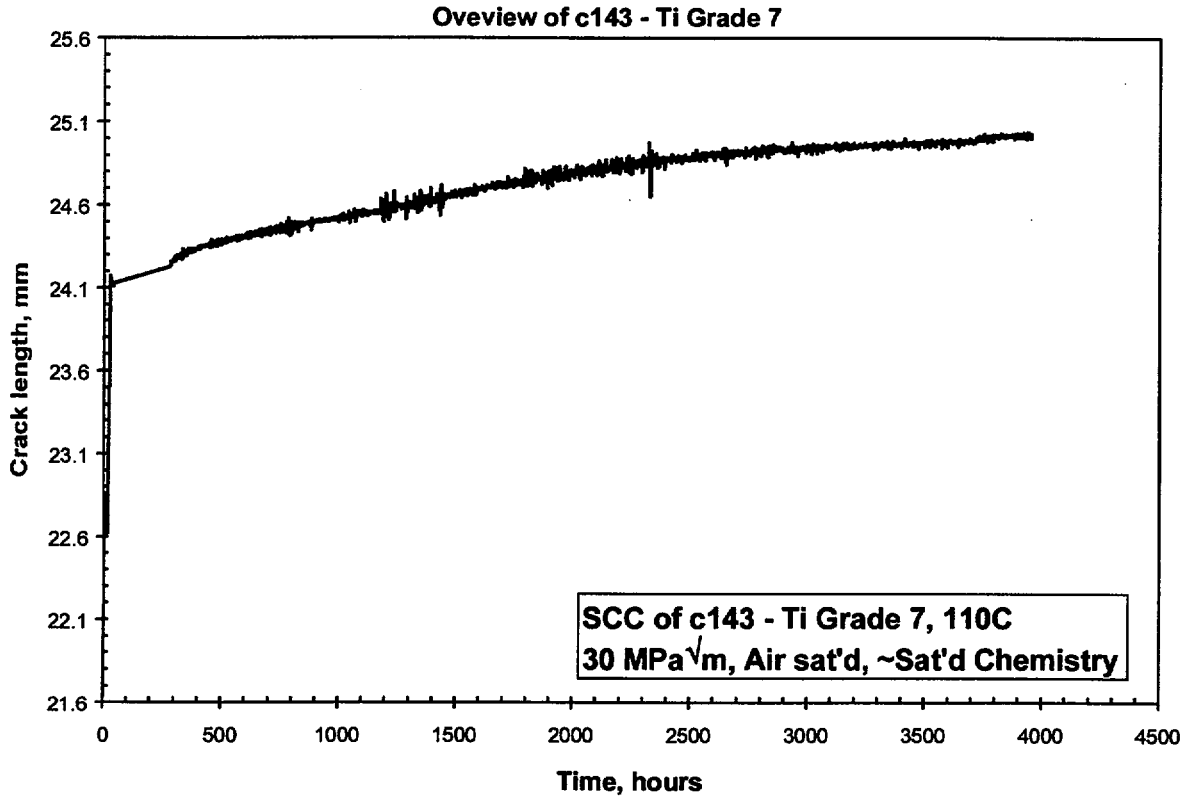

Figure 2. Overview of the air fatigue precracking and stress corrosion cracking testing of specimen c143 (titanium grade 7) at 110 °C in a concentrated mixed salt environment with 5 psi over-pressure of laboratory air.

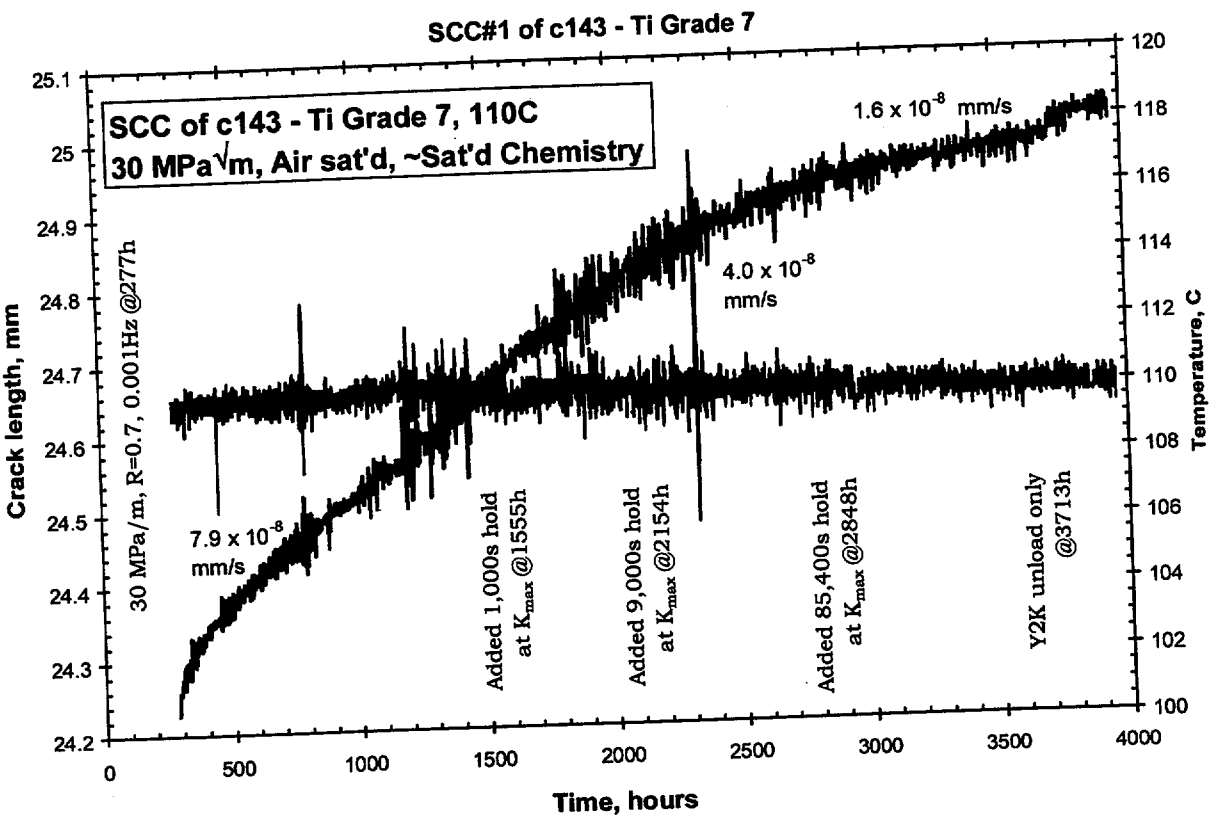

Figure 3. Crack length and temperature vs. time plot of the stress corrosion cracking response of specimen c143 (titanium grade 7) at 110 °C in a concentrated mixed salt environment with 5 psi over-pressure of laboratory air.

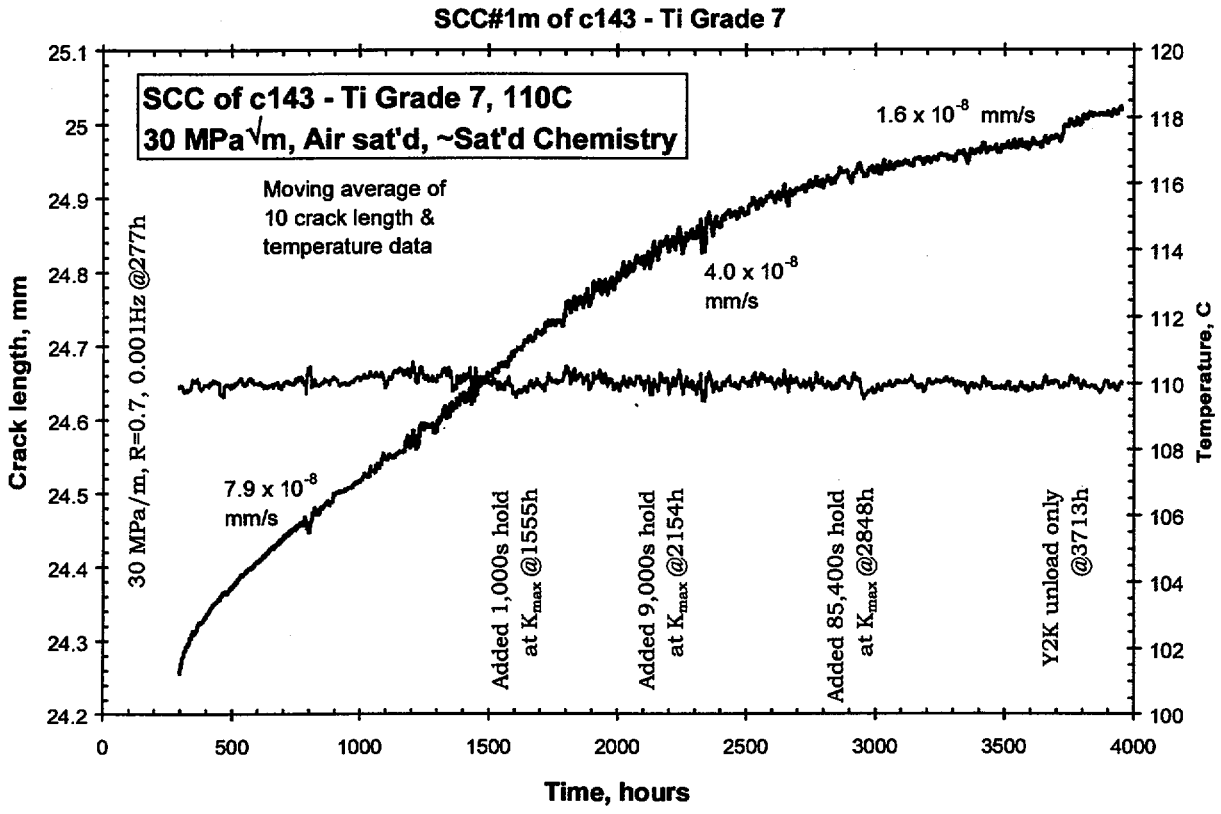

Figure 4. Crack length and temperature vs. time plot of the stress corrosion cracking response of specimen c143 (titanium grade 7) at 110 °C in a concentrated mixed salt environment with 5 psi over-pressure of laboratory air. A 10-point moving average was used to smooth the data, which proved quite sensitive to fluctuations in room and test (110 °C) temperature.

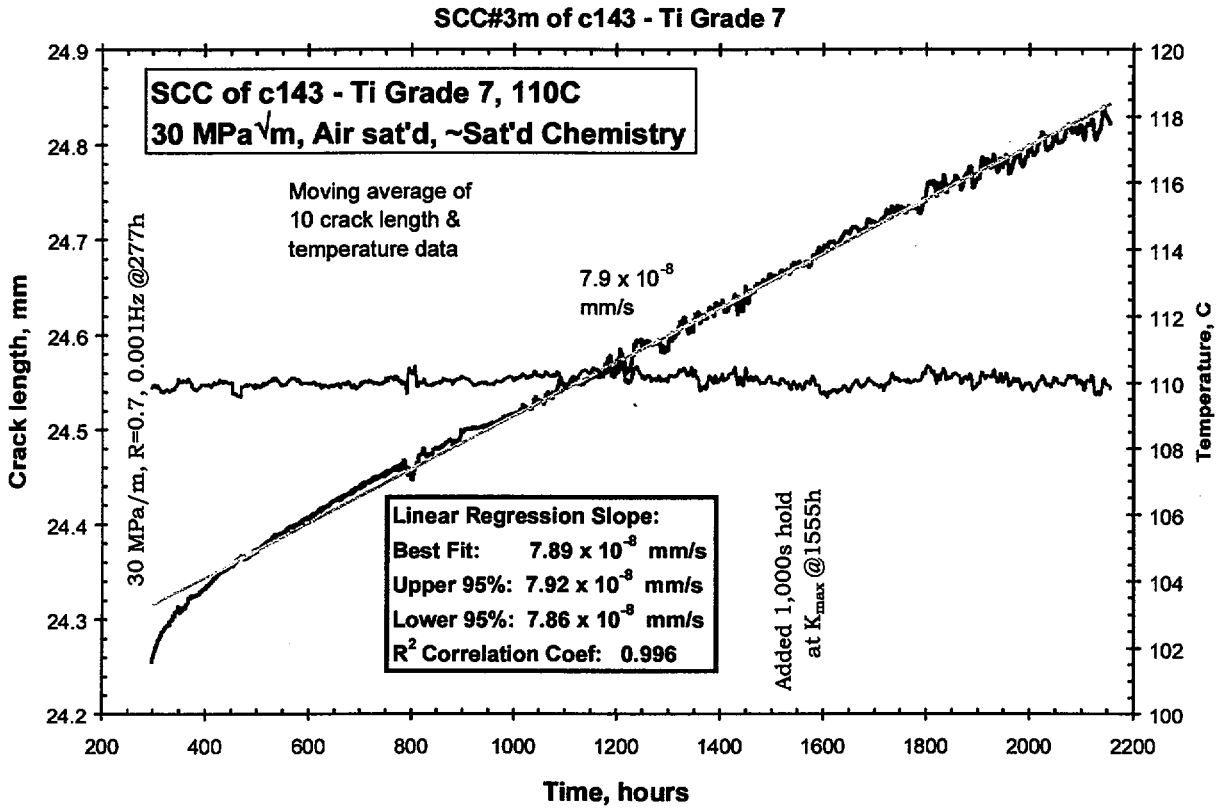

Figure 5. Crack length and temperature vs. time plot of the stress corrosion cracking response of specimen c143 (titanium grade 7) at 110 °C in a concentrated mixed salt environment with 5 psi over-pressure of laboratory air. The test interval of 297 to 2154 hours is shown, which corresponds to the period in which the loading was K_{max} = 30 MPa√m, R = 0.7, and 0.001 Hz. At 1555 hours, a 1,000 s hold at K_{max} was introduced. A 10-point moving average was used to smooth the data, which proved quite sensitive to fluctuations in room and test (110 °C) temperature.

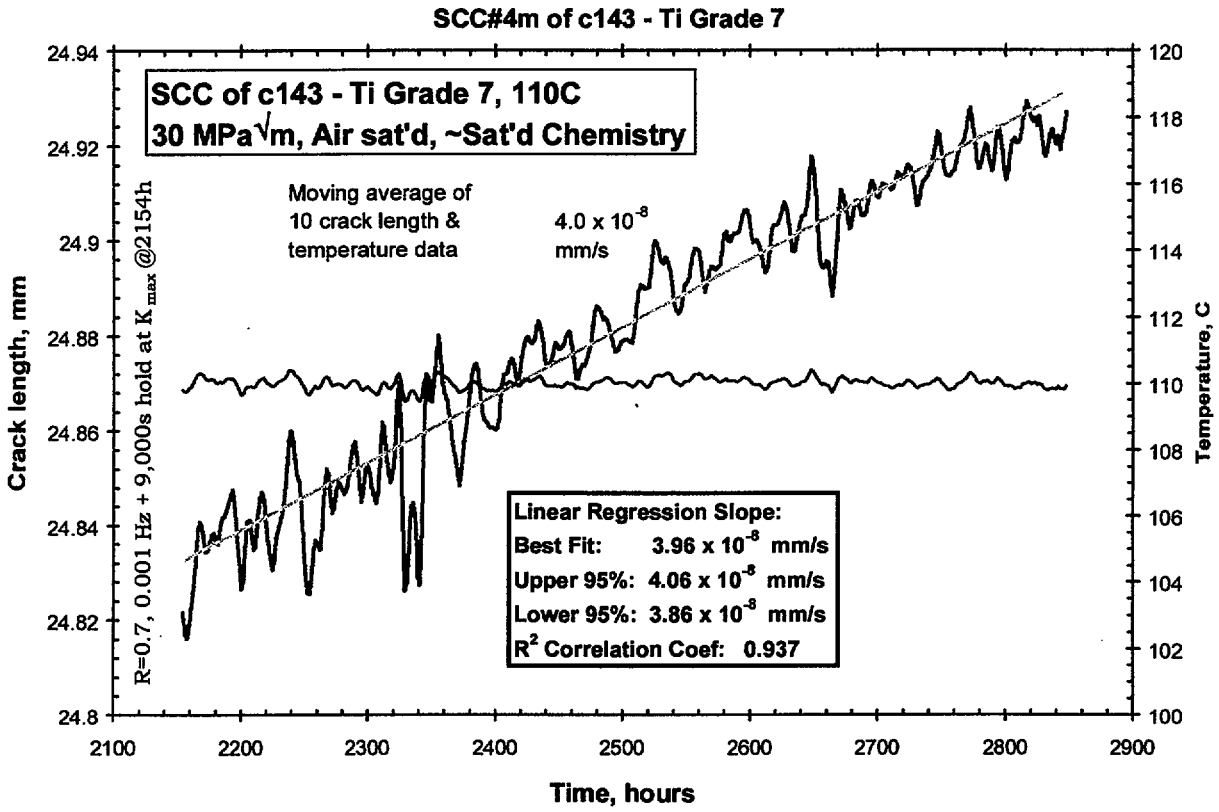

Figure 6. Crack length and temperature vs. time plot of the stress corrosion cracking response of specimen c143 (titanium grade 7) at 110 °C in a concentrated mixed salt environment with 5 psi over-pressure of laboratory air. The test interval of 2154 to 2848 hours is shown, which corresponds to the period in which the loading was K_{max} = 30 MPa√m, R = 0.7, and 0.001 Hz with a 9,000 s hold at K_{max}. A 10-point moving average was used to smooth the data, which proved quite sensitive to fluctuations in room and test (110 °C) temperature.

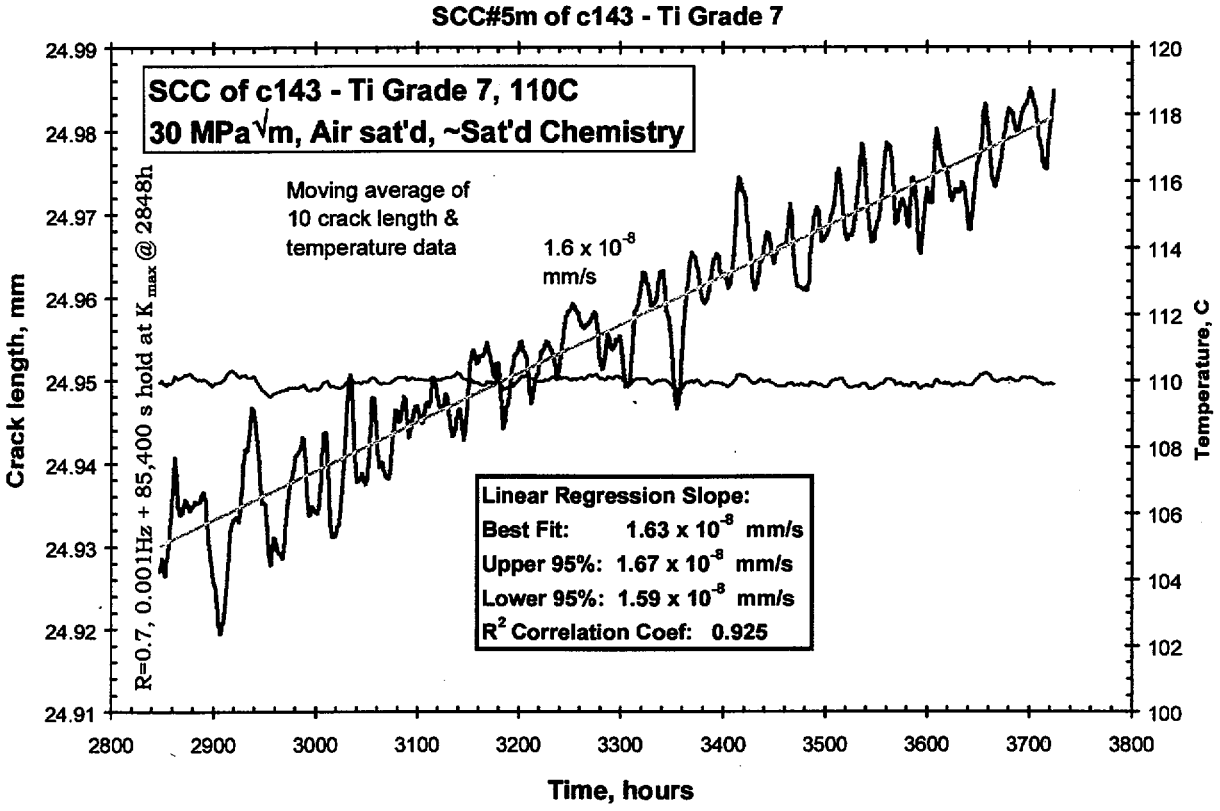

Figure 7. Crack length and temperature vs. time plot of the stress corrosion cracking response of specimen c143 (titanium grade 7) at 110 °C in a concentrated mixed salt environment with 5 psi over-pressure of laboratory air. The test interval of 2848 to 3724 hours is shown, which corresponds to the period in which the loading was K_{max} = 30 MPa√m, R = 0.7, and 0.001 Hz, with a 85,400 s hold at K_{max}. A 10-point moving average was used to smooth the data, which proved quite sensitive to fluctuations in room and test (110 °C) temperature.

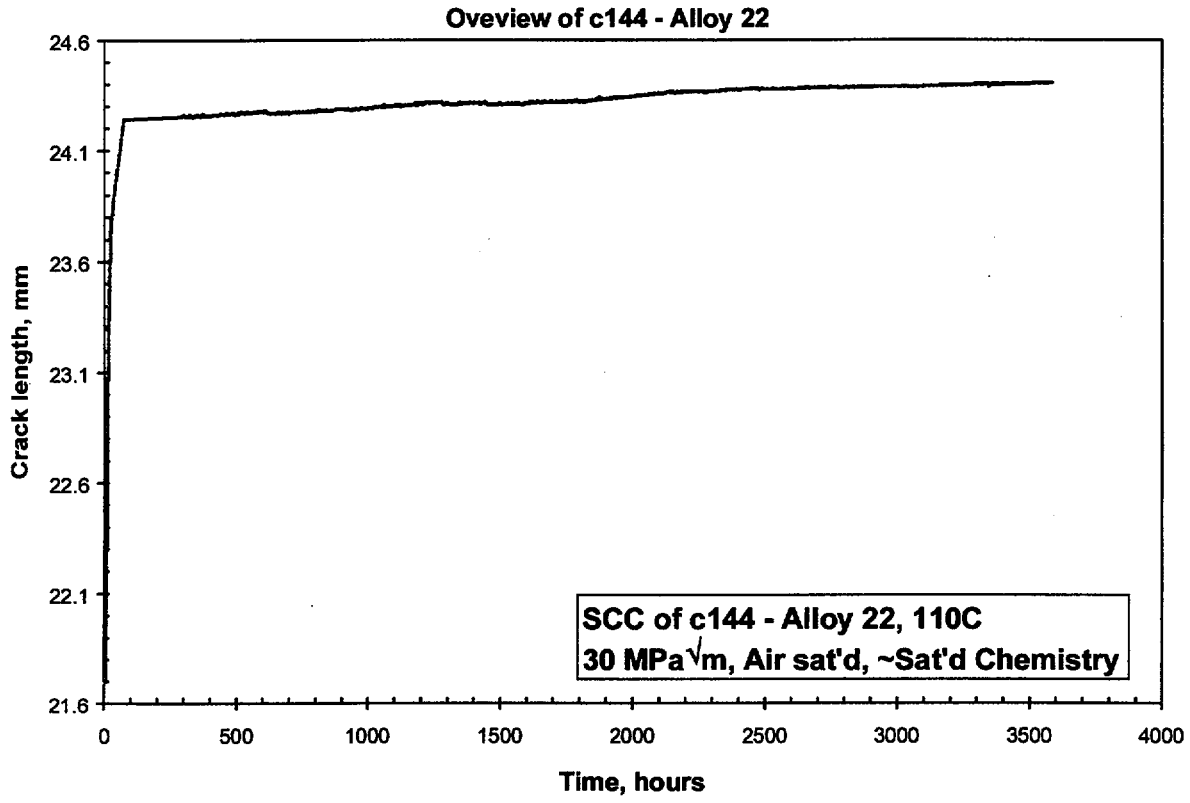

Figure 8. Overview of the air fatigue precracking and stress corrosion cracking testing of specimen c144 (Alloy C-22 base metal) at 110 °C in a concentrated mixed salt environment with 5 psi over-pressure of laboratory air.

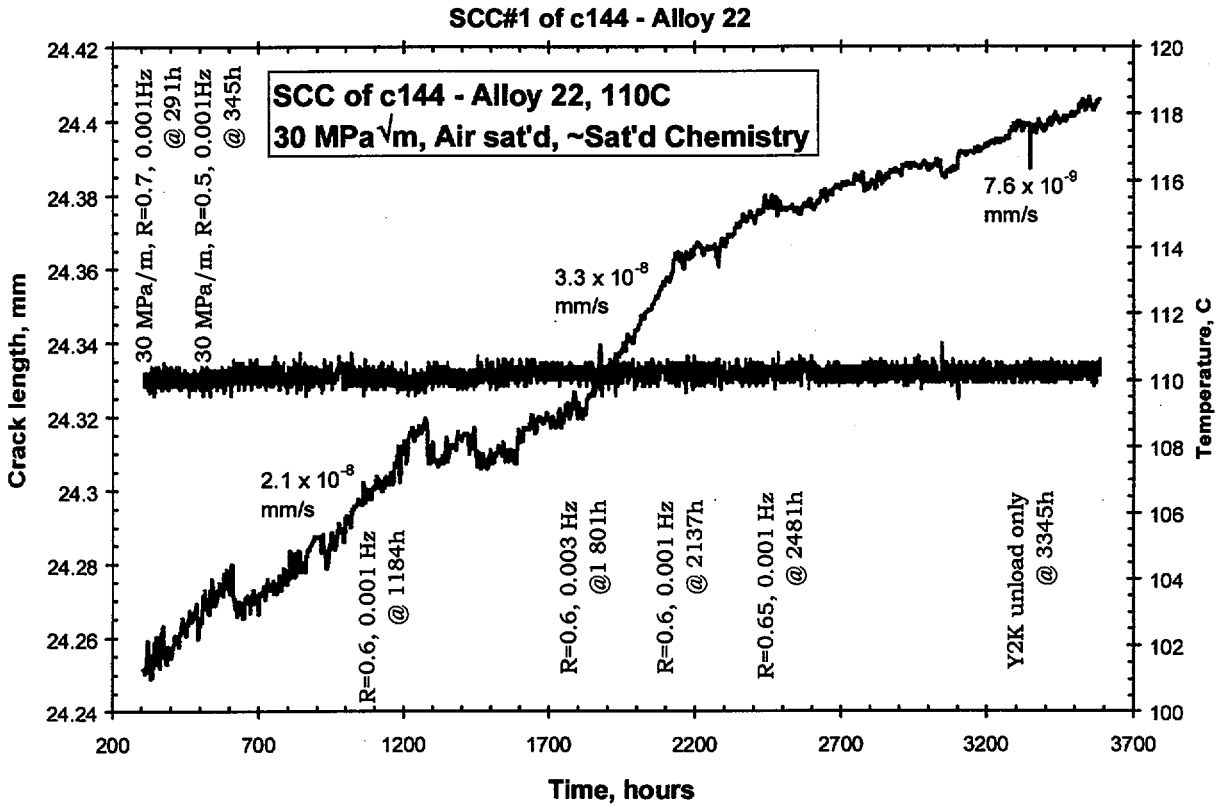

Figure 9. Crack length and temperature vs. time plot of the stress corrosion cracking response of specimen c144 (Alloy C-22 base metal) at 110 °C in a concentrated mixed salt environment with 5 psi over-pressure of laboratory air.

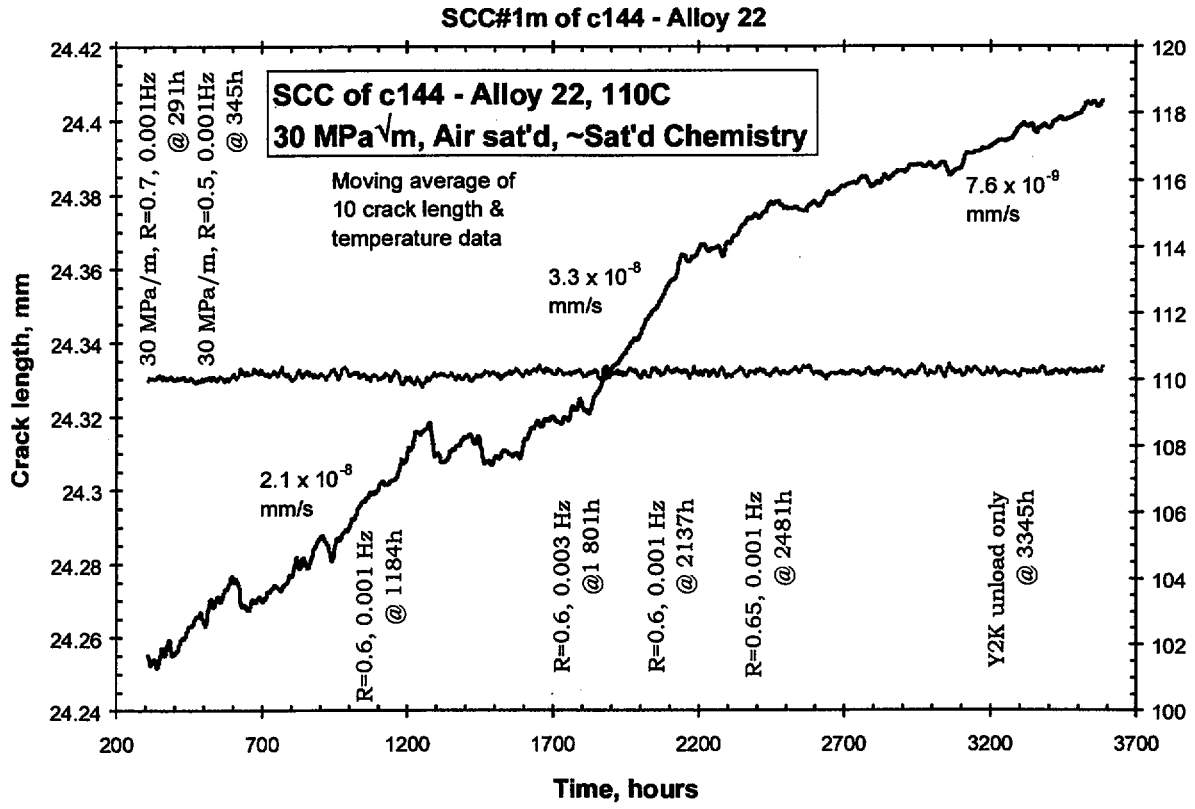

Figure 10. Crack length and temperature vs. time plot of the stress corrosion cracking response of specimen c144 (Alloy C-22 base metal) at 110 °C in a concentrated mixed salt environment with 5 psi over-pressure of laboratory air. A 10-point moving average was used to smooth the data, which proved quite sensitive to fluctuations in room and test (110 °C) temperature.

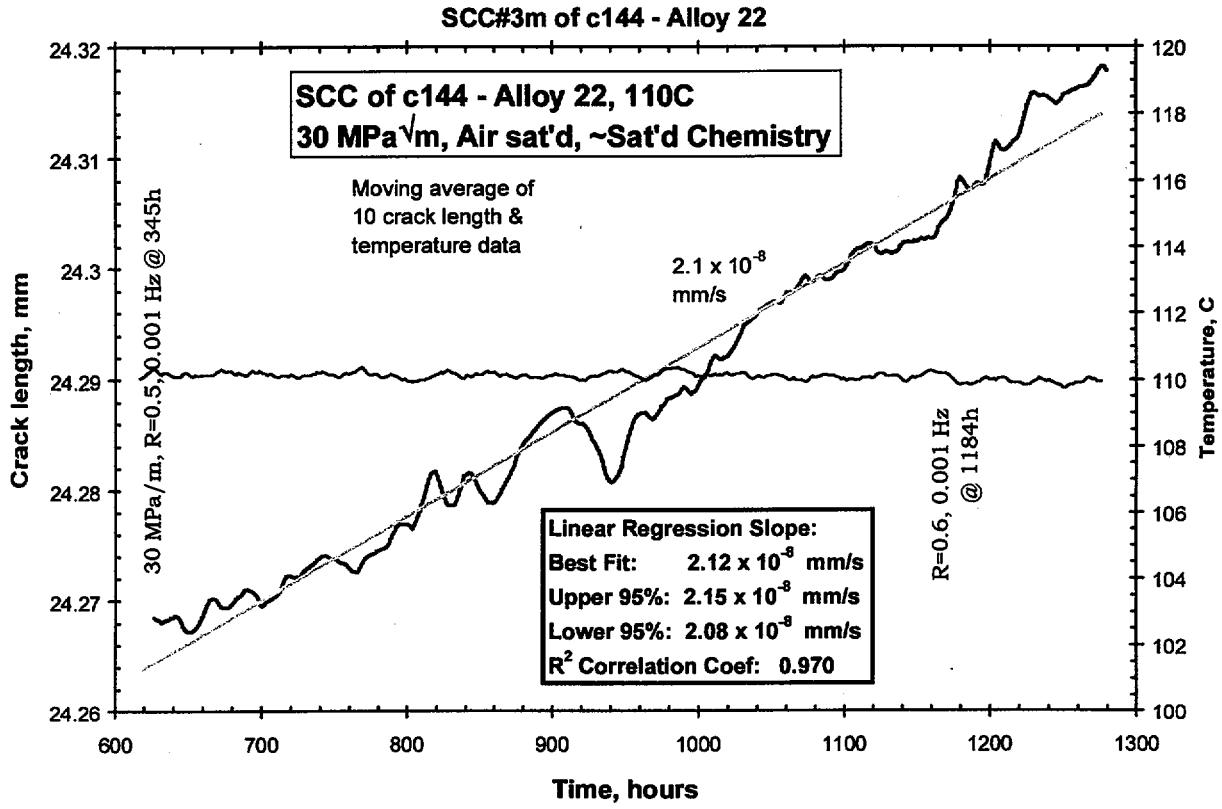

Figure 11. Crack length and temperature vs. time plot of the stress corrosion cracking response of specimen c144 (Alloy C-22 base metal) at 110 °C in a concentrated mixed salt environment with 5 psi over-pressure of laboratory air. The test interval of 629 to 1279 hours is shown, which corresponds to the period in which the loading was K_{max} = 30 MPa√m, R = 0.5, and 0.001 Hz. A 10-point moving average was used to smooth the data, which proved quite sensitive to fluctuations in room and test (110 °C) temperature.

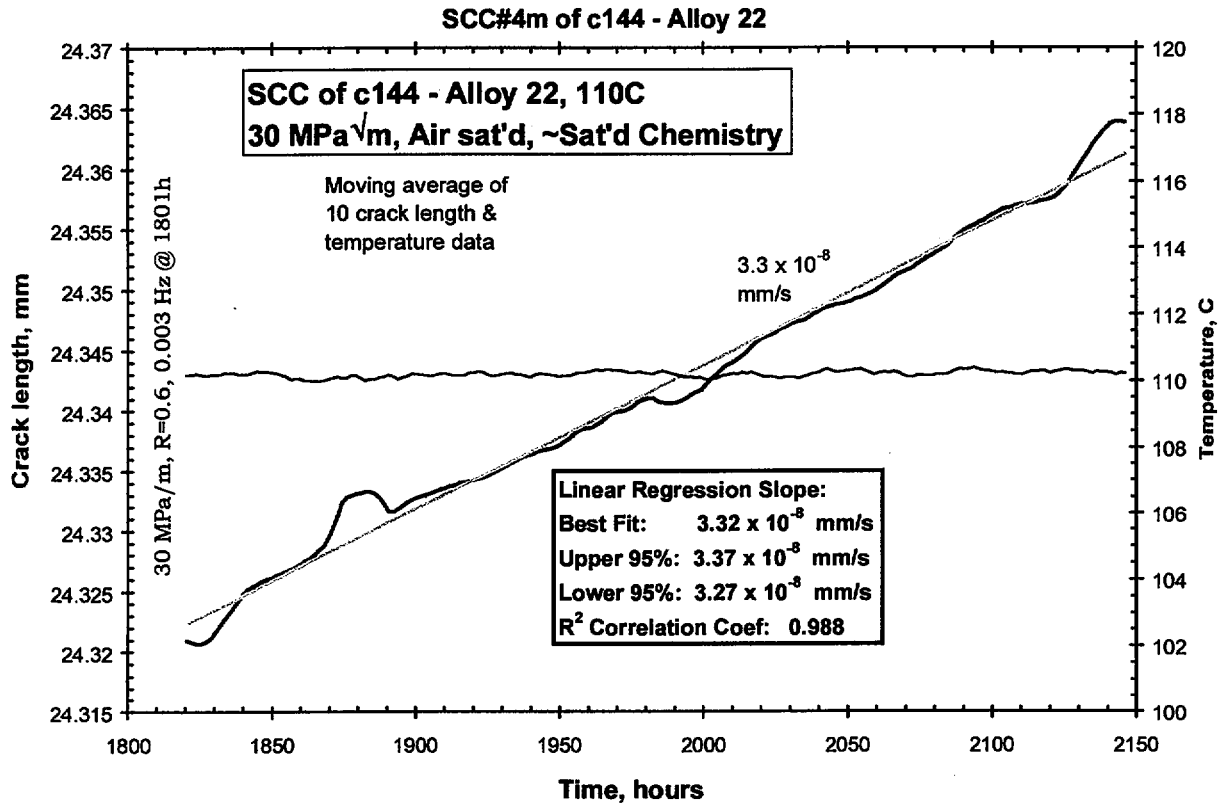

Figure 12. Crack length and temperature vs. time plot of the stress corrosion cracking response of specimen c144 (Alloy C-22 base metal) at 110 °C in a concentrated mixed salt environment with 5 psi over-pressure of laboratory air. The test interval of 1820 to 2146 hours is shown, which corresponds to the period in which the loading was K_{max} = 30 MPa√m, R = 0.6, and 0.003 Hz. A 10-point moving average was used to smooth the data, which proved quite sensitive to fluctuations in room and test (110 °C) temperature.

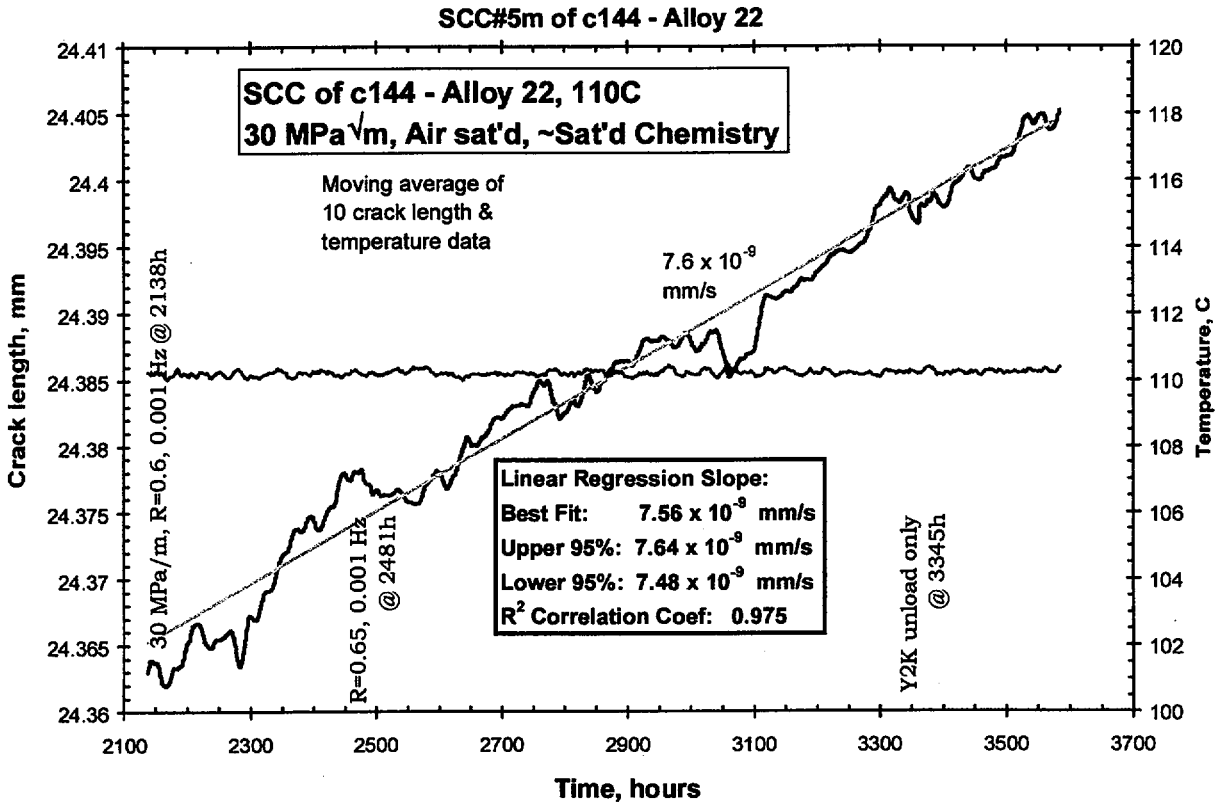

Figure 13. Crack length and temperature vs. time plot of the stress corrosion cracking response of specimen c144 (Alloy C-22 base metal) at 110 °C in a concentrated mixed salt environment with 5 psi over-pressure of laboratory air. The test interval of 2137 to 3585hours is shown, which corresponds to the period in which the loading was K_{max} = 30 MPa√m, R = 0.6 and R = 0.65, and 0.001 Hz. A 10-point moving average was used to smooth the data, which proved quite sensitive to fluctuations in room and test (110 °C) temperature.